Am J Transl Res 2020;12(10):6751-6762
www.ajtr.org /ISSN:1943-8141/AJTR0114776

Original Article

Evaluation of the clinicopathologic features of diffuse large B cell lymphoma after CD19-targeted CAR T-cell therapy emphasizing the potential diagnostic pitfalls

Jun Zhou[1*], Wenjing Zhang[1*], Yanping Zhang[2*], Saifang Zheng[1], Luting Zhou[1], Xiaoqun Yang[1], Chaofu Wang[1]

[1]Department of Pathology, Ruijin Hospital, Shanghai Jiaotong University School of Medicine, Shanghai, China; [2]Department of Pathology, The First Affiliated Hospital of Zhengzhou University, Zhengzhou, Henan, China. [*]Equal contributors.

Received May 22, 2020; Accepted October 1, 2020; Epub October 15, 2020; Published October 30, 2020

Abstract: Clinicopathologic data of 16 cases of DLBCL, NOS after CD19-targeted CAR T-cell therapy were retrospectively reviewed. Statistical analyses were performed to investigate the diagnostic agreement and indicate the relationship of the given types or their alterations (Group I versus Group II) to the prognosis. A total of 5 distinct histologic patterns were summarized. The CAR T cells were somewhat atypical, most of which were CD8 positive in the most cases (86.7%, 13/15), with a relatively high Ki-67 (60-90%). The rearrangement of BCR was demonstrated in all cases. The diagnostic test showed that the diagnostic accuracy in cases of types III (7%) and V (7%) was typically low; the diagnostic agreement in cases of type IV (for B, T, or nonlymphoma) and V (for T, or nonlymphoma) was consistently unsatisfactory. The rates of complete response (CR), partial response (PR), and progressive disease (PD) were 18.8% (3/16), 31.3% (5/16), 50% (8/16), respectively. In the follow-up, 25% (4/16) of cases experienced a recurrence and 31.3% (5/16) had died, of which 3 cases succumbed to the side effects. Group II had better disease-free survival (DFS, P=0.009). This study first described the pathologic features of DLBCL after CD19-targeted CAR T-cell therapy. Familiarity with these histologic features and combinations of medical history and genetic analyses facilitate avoiding misdiagnoses. Multiple biopsies are potentially helpful to estimate the treatment effects or prognosis, and stable alterations to any type of III to V, but not a single given one, may indicate a good prognosis.

Keywords: CAR T, clinicopathology, histologic pattern, misdiagnosis, pitfall

Introduction

Diffuse large B cell lymphoma (DLBCL) is the most common type of non-Hodgkin lymphoma worldwide [1]. DLBCLs are a clinically, morphologically and genetically heterogeneous group and include several subtypes or variants based on their distinct clinicopathologic features, molecular aberrations, or/and prognosis, among which the most majority fall into the category of DLBCL, not otherwise specific (DLBCL, NOS) [2]. Rituximab plus cyclophosphamide, doxorubicin, vincristine, and prednisone (R-CHOP) are the flagship treatments for DLBCL patients and have significantly improved the disease-free and overall survival during the last 20 years [3, 4]. However, approximately one-third of individuals will undergo refractory disease or relapses, and only a very limited fraction could be cured by otherwise aggressive salvage regimes followed by high-dose polychemotherapy and autologous stem-cell transplantation (ASCT) [4]. Increasing knowledge of some major genetic findings has facilitated the development of new therapeutic approaches, particularly based on the R-CHOP backbone [5, 6].

The emerging field of immunotherapy has massively progressed in the past decades, and hence, a subset of modalities has been adopted in clinical therapeutic practice [7]. Anti-CD19 chimeric antigen receptor (CAR) T-cell therapy, as a type of promising immunotherapy, utilizes autologous genetically engineered T cells designed for chimeric antigen receptors for targeting CD19-positive B cells [6]. This "breakthrough therapy" has shown remarkable efficacy in patients with B-cell acute lymphoblastic lymphoma (B-ALL) and has also demonstrated high efficacy for other relapsed/refractory

B-NHL, including the common type DLBCL, NOS, although is potentially associated with some unique toxicities [6, 8].

CD19-targeted CAR-T cell therapy has been applied to a few DLBCL subjects in large Chinese hospitals, whose therapeutic effects are not good by standard R-CHOP/CHOP, or similar schemes. We pathologists have encountered increasing numbers of submitted specimens from post CAR T-cell therapeutic patients. We found that the histomorphology may be variable for the different post-therapeutic cases due to their reactive extent. The large atypical B cells may not be prominent, which potentially obscures their neoplastic nature; or the substantial infiltration of atypical CAR-T cells is likely to raise a concern about a diagnosis of T cell malignancy. As yet, documented series to describe the concrete pathologic features have been lacking; hence, most pathologists are not familiar with these features, leading to potential erroneous diagnosis. As one of the top hospitals in China, we first collected the largest series of cases of DLBCL after CD19-targeted CAR T-cell therapy to summarize the general histologic features. Small-scale diagnostic tests among a few pathologists were also performed. All of that work aimed to enhance our knowledge of the distinctive morphologic correlates of post-CAR T cell therapy and to emphasize the potential diagnostic pitfalls for the pathologists in routine practice.

Materials and methods

Patients and case selection

This study was approved by the institutional board at the Department of Pathology, Ruijin Hospital, Shanghai Jiaotong University School of Medicine, and The First Affiliated Hospital of Zhengzhou University. Sixteen cases of DLBCLs with completed clinical data were included in our analysis, containing 13 cases from Ruijin Hospital and 3 cases from The First Affiliated Hospital of Zhengzhou University. All of the clinicopathologic features about both pre- and post-CD19-targeted CAR-T cell therapies from these 16 patients were recorded.

Pathologic evaluation, immunohistochemistry (IHC), and Epstein-Barr virus-encoded RNA (EBER) in situ hybridization (ISH)

All cases were independently reviewed by 2 senior pathologists (J.Z. and C.F.W.). The discernible morphologic changes/patterns compared to the pre-therapeutic hematoxylin and eosin (HE) sections were summarized and categorized. Each surgical specimen was specially re-sectioned. Four-micron-thick sections were taken from 10% formalin-fixed and paraffin-embedded tissue blocks followed by immunohistochemical staining using commercially available antibodies (all obtained from DAKO, Glostrup, Denmark, prediluted, except where indicated): CD20, CD79a, CD19, CD22, CD3, CD5, CD8, CD4, Bcl-2, CD30, CD21, CD10, BCL-6, Mum-1, c-myc, Ki-67. To simultaneously highlight CD20 and CD3, double staining was performed on some slides using a Leica *BOND-III* automated immunohistochemistry system (Leica Microsystems, Wetzlar, Germany). The primary antibodies were visualized using horseradish peroxidase (HRP) and alkaline phosphatase (AP), and the substrates were diaminobenzidine (DAB) and Fast Red, respectively (brown color for CD20 and red color for CD3). EBER ISH was detected on the paraffin section, performed using in situ hybridization kits (Dako, Carpinteria, CA, US) according to the manufacturer's instructions. The proportions of B and T cells and the positive rates of CD8, CD4, Granzyme B, TIA-1, and CD30 were recorded in 5% increments.

B- and T-cell receptor (B/TCR) rearrangement analysis

BCR and TCR gene rearrangement analyses were carried out with polymerase chain reaction (PCR) to detect B cell clonality by testing for immunoglobulin heavy chain (IGH) and Kappa light chain (IGK) genes. T cell clonality was evaluated by testing for TCRβ (TCRB), TCRδ (TCRD), and TCRγ (TCRG). A Gene Clonality Assay Kit (InVivoScribe Technologies, San Diego, CA) was applied in this study, and products were then separated by capillary electrophoresis using an ABI 3500 automatic sequencing system (Applied Biosystems Invitrogen, Foster City, CA, US) followed by analysis with GeneScan Analysis Software (Applied Biosystems Invitrogen).

Diagnostic tests and results analysis

To investigate the frequency and potential misdiagnoses for cases after CD19-targeted CAR T-cell therapy, five senior pathologists from Ruijin Hospital were randomly selected to make a diagnosis for these 16 cases. A total of 19

slides entered the tests containing all 5 histologic types (Types I and II, n=5, respectively; III, IV, V, n=3, respectively). Note 2 different slides of Type IIII were derived from the same case to increase its test number due to the statistical need. All of clinicopathologic and IHC data were offered in the setting of unawareness of the history of treatments as well as molecular outcomes. All the diagnostic results were recorded, and the total accuracy in each histologic Type was calculated. The diagnostic agreements for the diagnosis of B cell lymphoma, T cell lymphoma, and nonlymphoma were analyzed in each histologic type through Fleiss' kappa statistics using SPSS version 22 (IBM SPSS Statistics Inc., Chicago, US). The diagnostic agreements were interpreted by the kappa value according to previously published literature [9]: <0, no; 0.0-0.19, poor; 0.20-0.39, fair; 0.40-0.59, moderate; 0.60-0.79, substantial; 0.80-1, almost perfect.

Follow-up and statistical analysis

Follow-ups were performed in the office setting or by telephone interview. The relationship between each histologic type and the prognosis (alive with disease [AWD] without progression, versus progression to recurrence or death) within our follow-up duration were analyzed using the Chi-Square test. In addition, to indicate the prognosis involved by different alterations of histologic types, the data from patients with multiple biopsy results was submitted to univariate survival analysis. The analyzed patients were divided into two groups according to changes in the histologic pattern until the end of our follow-up: any histologic patterns eventually grow into I or II type (Group I) or into any of III-V types (Group II). Rather than OS, DFS (disease-free survival) was statistically calculated due to the relatively short follow-up duration in our series. Kaplan-Meier curves of the DFS curves were plotted and compared by log-rank test. $P<0.05$ in all analyses was considered as statistically significant. The statistical analysis was performed with SPSS v. 22.0 (IBM SPSS Statistics Inc., Chicago, US).

Results

Clinical features

The main clinical features of the 16 cases are summarized in **Table 1**. These patients included 12 males and 4 females (male to female ratio: 1:0.33), ranging in age from 27 to 63 years (mean, 48.4 yr.; median, 50.5 yr.), 3 of whom had a family history of DLBCL (case 2, 4, 5). Most patients complained of enlarged lymph nodes at distinct locations with or without extranodal involvement of organs or tissues; only 3 patients initially presented with retroperitoneal (case 10), jejunal and pancreatic (case 12), or testicular (case 14) occupying lesions. Definite bone marrow involvement was confirmed by pathologic biopsy in 3 cases. Half (8/16) demonstrated B symptoms, that is, fever (4/8), night sweats (5/8), or weight loss in a short period (2/8). Almost all the patients showed elevated serum lactic dehydrogenase (17/17) or beta-2 microglobulin (B2M; 6/13). Based on the clinical features above, the International Prognostic *Index* (IPI) of our cases was generally unfavorable (6.3% [1/16] with IPI of 1, 25% [4/16] with IPI of 2, 68.7% [11/16] with IPI of 3-4). All the cases were uniformly staged according to the Ann Arbor staging system, with 43.8% (7/16) of early stage (I/II) and 56.2% (9/16) of advanced stage (III/IV). All the patients received the conventional R-CHOP therapy, among which 62.5% (10/16) did not respond to the regimen, 25% (4/16) progressed after the partial response (PR), and 12.5% (2/16) relapsed after a complete response (CR). All subjects underwent 5 days of fludarabine and cyclophosphamide chemotherapy followed by an infusion of CAR T-cell infusion (axicabtagene ciloleucel [axi-cel]). Overall, 75% of our series only received one round of CAR T-cell treatment, and the remaining 25% underwent two cycles of therapy with variable intervals (range, 6 to 60 days; mean, 34.3 days; median, 45 days).

Histologic features

The morphology of 16 cases before CAR T-cell therapy is compatible with the diagnosis of DLBCL, NOS. They typically showed diffuse destructive infiltrate by large neoplastic B cells in lymph nodes or extranodal sites, some associated with very few reactive T cell lymphocytes or fibrous deposition. For the counterparts after CAR T-cell therapy, we summarized 5 principal histologic patterns according to our observations: Type I, neoplastic B cell predominance featuring large sheets of atypical large B cells with very limited T cell infiltration with or with-

Table 1. Clinicopathologic features of 16 cases of DLBCL receiving CD19-targeted CAR T-cell therapy

Case No.	Age (yr.)/ Sex	Biopsy Site	Presentation	B symptoms	BW Involvement	High LDH/ B2M	IPI Score	Stage	Hans' Classification	Therapeutic No./Interval (dy.)	Duration from biopsy to CAR-T cell therapy (dy.)/No.	Therapeutic effect	Outcome (mo.)
1	56/M	LN	Mass in right groin with ipsilateral lower limb swelling; bilateral pelvic enlarged lymph nodes	N	N	Y/N	4	IIEA	non-GCB	1/-	11, 18/2	CR	AWD (23)
2	32/M	LN	Progressive enlarged lymph nodes in left neck and right pulmonary hilum; cough and expectoration; fever	Y	N	Y/N	1	IIA	GCB	1/-	8, 18/2	PR	AWD (20)
3	56/F	LN	Mass in left neck	N	N	Y/N	2	IIIEA	GCB	1/-	16/1	PR	AWD (16)
4	63/F	LN	Enlargement in left groin with abdominal distending and paroxysmal pain; weight loss	Y	N	Y/Y	4	IVB	non-GCB	1/-	8, 61, 90, 152/4	PR followed PD	Recurrence (12)
5	57/M	LN	Enlarged submandibular and neck lymph nodes during PE	N	N	Y/N	3	IIA	non-GCB	1/-	108, 109, 110/3	PR followed by PD	Recurrence (4)
6	61/F	LN	Multiple lymph node enlargement; fever and night sweat	Y	N	Y/Y	2	IIB	GCB	1/-	180/1	PD	Dead (6)
7	46/F	LN	Right enlarged tonsil and abdominal pain; night sweat	Y	N	Y/Y	4	IB	non-GCB	2/41	12, 28/2	PD	Dead (2)
8	46/M	LN	Mediastinal, left axillary, pancreatic, splenic mass; dyspnea	N	Y	Y/N	3	IIIA	GCB	2/60	8/1	PD followed by PR	AWD (9)
9	40/M	LN	Multiple enlarged lymph nodes; right testicular swelling; pain in right shoulder; fever	Y	N	Y/Y	3	IIEA	non-GCB	1/-	15, 85/2	PD	Recurrence (12)
10	51/M	RP	Retroperitoneal mass; cough, waist complaints; fever	Y	N	Y/Y	4	IVB	GCB	1/-	49/1	PR	AWD (6)
11	57/M	LN	Enlarged lymph nodes in left neck; weight loss, night sweat	Y	N	Y/N	3	IIIS	non-GCB	1/-	8, 53/2	PR	Recurrence (16)
12	50/M	Jejunum, pancreas	Occupying lesions in jejunum and pancreas; abdominal swelling, back pain	N	N	Y/N	2	IIE	non-GCB	2/30	383/1	CR	AWD (20)
13	44/M	LN	Left inguinal and right neck swelling; mass in nasal cavity, right testis and adrenal gland; night sweat	Y	N	Y/NA	3	IVB	GCB	1/-	189/1	CR	AWD (24)
14	54/M	Testis	Mass in bilateral testes, left kidney and right buttock	N	N	NA/NA	4	IVA	non-GCB	1/-	8, 15/2	PD	Dead (1)
15	35/M	LN	Right abdominal, pelvic and intestinal mass	N	Y	Y/Y	3	IVA	non-GCB	1/-	8, 20/2	PD	Dead (1)
16	27/M	LN	Mass in left head neck; involvement in bone marrow and CSF	N	Y	Y/NA	2	IVA	non-GCB	2/6	12/1	PD	Dead (1)

AWD, alive with disease; BW, bone marrow; LN, lymph node; RP, retroperitoneum; PE, physical examination; N, no; Y, yes; d, day; CR, complete response; PR, partial response; PD, progressive disease; NA, not available; dy, day; mo, month; CFS, cerebrospinal fluid.

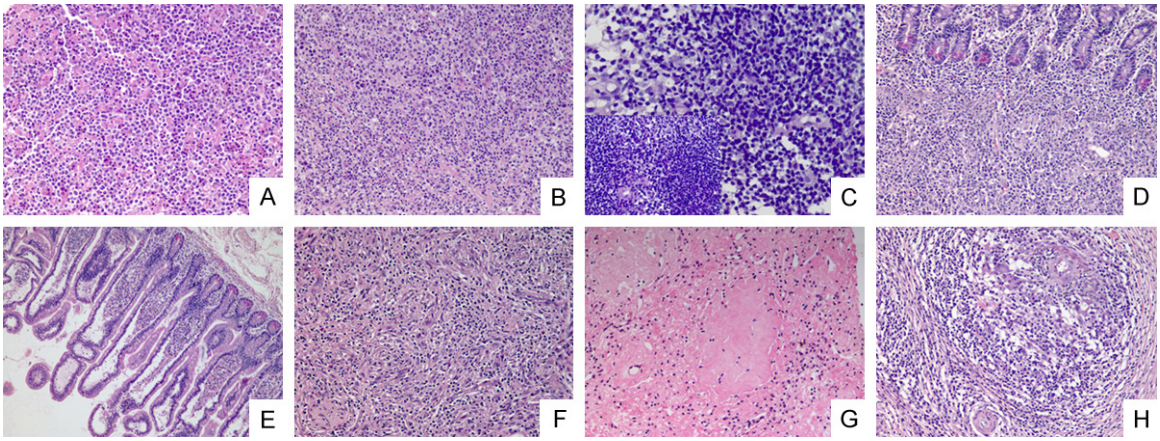

Figure 1. Representative features of the 5 histologic types of DLBCLs after CD19-targeted CAR T-cell therapy. Type I: diffuse large B cell infiltration with hardly an appreciable and very scattered T cells, indicating that the tumor cells are still dominant in this setting (A); type II: large neoplastic B cells intermingled with atypical T cells with focal T-cell rosette formation, representing the interaction between the tumor cells and CAR T-cells (B); type III: diffuse infiltration of atypical T cells with very few B cells, which is hardly appreciable, suggesting the CAR T-cells prevail in this setting (C), and the T cells may be slightly atypical, characterized by irregular and elongated nuclei with a small amount of cytoplasm (inset in C); note an intestinal case showing a diffusely transmural infiltration by atypical T cells (D, type III) with mucosal enteropathy-like changes, mimicking MEITL (E); type IV: vague nodules delineated by variably proliferated fibroblasts and histocytes with scattered atypical T cells (F); type V, prominent fibroblastic (not shown) or collagenous stroma with variably scattered T cells (G). Angiodestruction by T cells may be appreciated, particularly in the extranodular cases; this histologic feature, though frequently seen in the aggressive lymphohematopoietic diseases, does not indicate its malignant nature in the setting of CAR T-cell therapy (H). However, none of the types described above can predicate the development of the whole disease and the patient's prognosis, though determining the variations of different types from multiple biopsies is warranted.

out coagulative necrosis; Type II, neoplastic B cells intermixed with T cells, the latter accounting for >10% of all cells; Type III, T cell predominance featuring diffuse T cell infiltration with very few (≤10% of all cells) neoplastic B cell components; Type IV, granuloma-like pattern characterized by nodular aggregation of T cells and proliferated fibroblasts; Type V, fibrotic pattern characteristic of widely proliferated fibroblasts with varying extents of T cell infiltration and collagen deposition. Cases were assigned to a given type according to their main growth pattern, though coexisting patterns were not uncommon.

Among the biopsies after the initial CAR T-cell therapy, the most majority of tissues evaluated were core needle biopsy, except for 1 case of intestinal resection (case 12) and 3 lymphadenectomies (case 14-16). In total, 31.3% of cases (5/16) corresponded to Type 1 (**Figure 1A**), of which 2 cases were associated with prominent neoplastic coagulative necrosis. Additionally, 31.3% (5/16) were Type II, with unorganized sheets of large B cells intermingled with T cells with or without more or less polymorphonuclear cells, histocytes, and fibroblasts; focal presence of prominent T-cell rosettes surrounding neoplastic B cells (case 2, **Figure 1B**) or pattern of type IV (case 3) could be appreciable in some cases. Only 2 cases (12.5 %) in our group were Type III (**Figure 1C**), of which 1 case (case 12, **Figure 1D**) involved the intestine showing diffuse transmural infiltration by atypical T cells with superimposed mucosal enteropathy-like changes, namely, villous atrophy, crypt hyperplasia as well as increased intraepithelial lymphocytes mimicking monomorphic epithelial intestinal T-cell lymphoma (MEITL, **Figure 1E**); focal necrosis could be seen. Another 2 cases (12.5%) of Type IV consisted of scattered T cells and vague nodules delineated by variably proliferated fibroblasts with or without residual nested B cells in their epicenters (**Figure 1F**). Diffuse proliferated fibroblasts or prominent collagenous stroma with variably scattered T cells tended to obscure the small residual B cell clusters in the remaining 2 cases (12.5%) of Type V (**Figure 1G**); one of them (case 9) focally presented with pattern IV. The infiltrated T cells in most cases above cytologically showed mild to moderate atypia

Table 2. Components of lymphocytes, genetic analyses in the first biopsy and changes of histologic pattern (if any) after CD19-Targeted CAR T-cell therapy

Case No.	Proportion* (B/T, %)	Positive rate of T cells (%)						BCR/TCR	Histologic patterns
		CD8	CD4	Granzyme B	TIA-1	CD30	Ki67		
1	50/50	90	0	0	60	0	60	+/-	II, V
2	60/40	80	5	0	80	0	80	+/-	II, IV
3	50/50	50	50	5	10	0	80	+/-	II
4	90/10	80	0	10	80	0	70	+/-	I, V, IV, II
5	55/45	90	0	5	80	0	90	+/-	II, I, I
6	95/5	90	5	0	50	0	90	+/-	I
7	5/20	80	5	0	5	0	60	+/-	V, I
8	95/0	0	0	0	0	0	0	+/-	I
9	10/40	80	5	0	70	0	80	+/-	V, I
10	95/5	80	0	0	80	0	90	+/-	I
11	5/50	80	5	60	80	0	60	+/-	IV, I
12	5/95	60	40	5	60	0	60	+/-	III
13	0/95	90	5	0	80	0	70	+/-	III, IV
14	10/50	80	10	0	70	0	75	+/-	IV, I
15	55/45	50	5	0	80	0	80	+/-	II, I
16	95/5	90	0	0	90	0	80	+/-	I

*, the proportion of B or T cells among the aggregates of B and T cells, respectively.

featuring irregular and elongated nuclei with a small amount of cytoplasm (inset in **Figure 1C**). Focal invasion of intact glands (lymphoepithelial lesions LEL) and angiodestruction by T cells were frequently appreciated, particularly in the extranodular cases (**Figure 1H**). A second biopsy for 5 cases was taken at distinct intervals after treatment due to clinical suspicion of recurrence or progress (**Tables 1**, **2**). They mostly evolve into the presence of large quantities of B cells represented by a histologic transformation from type II (case 5), IV (case 11, 14), or V (case 7, 9) to type I. One case (case II) regressed from type II to type IV, with focal necrosis and a multinuclear giant cell reaction. Another one (case 4) underwent multiple biopsies for the purpose of pathologically monitoring disease changes, who presented with a fluctuation from type I to V to IV, and again to II, backward.

Immunohistochemical features and genetic analysis

A total of 62.5% (10/16) cases in this series were *germinal* center B-cell (*GCB*) and 37.5% (6/16) were non-GCB according to Hans' Classification through an immunohistochemical combination of CD10, BCL-6, and Mum-1 [10]. The neoplastic B cells of all cases were typically positive for CD19, CD22, CD20, CD79a, and the T cells were labeled with CD3 (**Figure 2A**) and CD5. The absence of follicular dendritic meshworks was confirmed by CD21 in all cases. The concrete proportion and immunochemical features for T cells of the first biopsy after CAR T-cell therapy are summarized in **Table 2**. The proportions of B (range, 0 to 95%; mean, 48.4%; median, 52.5%) and T cells (range, 0 to 95%; mean, 37.8%; median, 42.5%) in all cells varied according to different histologic types (**Figure 2B**), of which, the ratio of B to T cells was usually higher in Type I-II than in Type III-V. The majority of infiltrative T cells were labeled by CD8 in most cases (86.7%, 13/15, **Figure 2C**), with positive rates ranging from 50 to 90% (mean, 78%; median, 80%). Much fewer expressed CD4 (range, 0 to 50%; mean, 9%; median, 5%); however, 2 (case 3, 12) of these cases were almost equal in the numbers of B and T cells (**Figure 2D**). Most cases showed high positive rates of TIA (range, 5 to 90%; mean, 65%; median, 80%; **Figure 2E**), but only a few were positive for Granzyme B (range, 0 to 60%; mean, 5.7%; median, 0%; **Figure 2F**), and all T cells were negative for CD30. The proliferative index Ki-67 was relatively high, ranging from 60 to 90% (mean, 74.7%; median, 80%; **Figure 2G**). EBER was not detected in any cases in our series. The clonal rearrangement of BCR

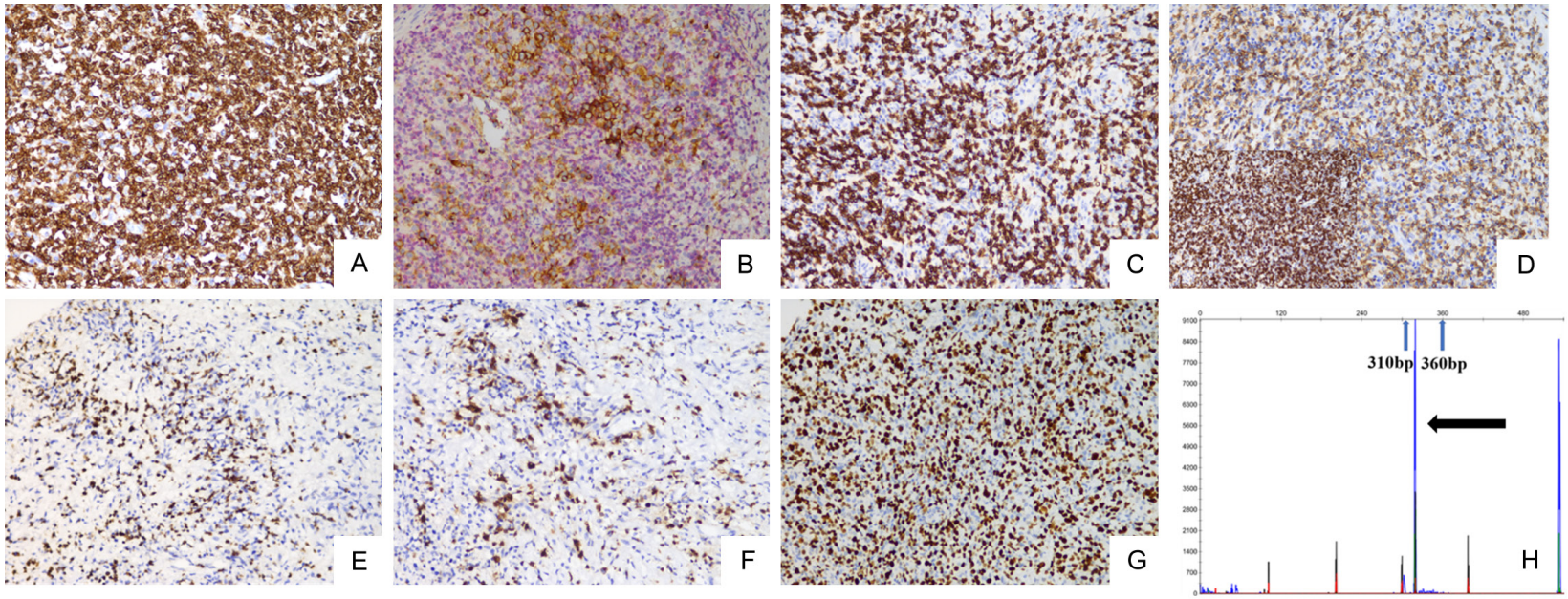

Figure 2. Immunohistochemical features of DLBCLs after CD19-targeted CAR T-cell therapy. The infiltrated atypical T cells were positive for CD3 (type I, A); double staining (type II) showed mixed B and T cells, labeled by CD20 (brown) and CD3 (red), respectively; the close mixture of these two cell components further indicates the process of their mutual interaction (B); the majority of atypical T cells were positive for CD8 (C) but negative for CD4 (not shown) in our series; a subset of cases showing a mixed proportion of atypical T cells immunoreactive for CD4 (D) or CD8 (inset in D) (type III); this type IV case showed that almost all of the scattered T cells were positive for TIA-1 (E), but only a few cases demonstrated a few T cells expressing granzyme B (F, type IV); the proliferated index Ki-67 was typically high for the T cells (G, type II; note: the darker staining of large B cells was also labeled here); a representative case here showing a single blue peak (arrow) falling in the 310-360 bp region suggestive of a monoclonal rearrangement of Ig H (H).

Table 3. Diagnostic results, accuracy and agreements for all 5 histologic types by 5 selected senior pathologists

Histologic Types	No. of Types	Lymphoma		Nonlymphoma n (%)	Diagnostic accuracy (%)	Diagnostic agreement for dx. of BCL Kappa	Diagnostic agreement for dx. of TCL Kappa	Diagnostic agreement for dx. of nonlymphoma Kappa
		TCL n (%)	BCL n (%)					
I	25	0 (0)	25 (100)	0 (0)	100	1	1	1
II	25	1 (4)	23 (92)	1 (4)	92	0.680	0.840	0.840
III	15	13 (87)	1 (6)	1 (6)	7	0.733	0.467	0.733
IV	15	5 (33)	3 (20)	7 (47)	20	0.196	-2.000	-2.000
V	15	2 (13)	1 (7)	12 (80)	7	0.600	0.333	-0.067

was consistently observed in all the cases (**Figure 2H**), but none showed a restriction of TCR.

Diagnostic test findings

The diagnostic tests and agreement results for the diagnosis of B cell lymphoma (BCL), T cell lymphoma (TCL), and nonlymphoma in each histologic type are summarized in **Table 3**. All 5 pathologists came to a diagnostic agreement in the slides of type 1 (kappa =1, for dx. of BCL, TCL, and nonlymphoma), with 100% accuracy. A moderate (kappa =0.680, for dx. of BCL) or substantial (kappa =0.840, for dx. of both TCL and nonlymphoma) diagnostic agreement was reached in cases of type II, but only one slide from the recurrent case (case 4) showing a relatively increased ratio of T to B cells was not readily interpreted as BCL by 2 pathologists (misdiagnosed as TCL and nonlymphoma, respectively). Notably, the majority of cases of type III were misdiagnosed as TCL (87%), leading to a very low diagnostic accuracy (7%), but relatively uniform diagnostic agreement (Kappa =0.733, 0.467, 0.733, for dx. of BCL, TCL, and nonlymphoma). Not only did the pathologists have difficulty making a correct diagnosis of BCL in the cases of both type IV and V (diagnostic accuracy, 20%, and 7%, respectively) but also no or poor diagnostic agreement was demonstrated (type IV: Kappa =0.196, -0.200, -0.200 in dx. of BCL, TCL, and nonlymphoma, respectively; type V: Kappa =0.300, -0.067 in dx. of TCL, and nonlymphoma, respectively), except for the diagnosis of BCL in type V, which had moderate agreement (Kappa =0.600). However, all 5 pathologists changed their primary diagnosis to DLBCL when they were informed of the patients' histories of treatments and molecular outcomes.

Treatment effect, follow-up and statistical analysis

The therapeutic response was clinically assessed by the physical examination and contrast-enhanced computed tomography (CT) and positron emission tomography (PET) scans. As depicted in **Table 1**, 14 biopsies (51.9%, 14/27) were aimed at providing a pathologic evaluation of the treatment effects after CAR-T cell therapy, whereas the remaining biopsies were taken in part because for re-assessment in cases of recurrence or progress of DLBCLs. Three patients (18.8%) achieved a complete response (CR), corresponding to patterns II (1/3) and III (2/3) in histologic type in their first biopsies. Five individuals (31.3%) had a partial response (PR), including 1 case with the previous state of progressive disease (PD); their histologic types included types I (42.9%, 3/7), II (28.6%, 2/7), and IV (28.6%, 2/7). Eight cases (50%) presented with PD, including previous PR in 2 cases (cases 4, 5); their histologic types included types I (43.8%, 7/16), II (25%, 4/16), IV (12.5%, 2/16), and V (18.8%, 3/16). Among the 5 histologic patterns in the initial biopsies, only patients with type III (100%, 2/2) acquired CR; others did not show a significant association with the given long-term treatment effects. In the 10 patients who underwent multiple biopsies, 3 cases experienced their histologic patterns from type II (case 1, 2) or III (case 13) up to type IV (case 2 and 13) or V (case 1), acquiring a long-term CR (case 1 and 13) or PR (case 2). Another 6 cases went through the variations from other types (type II, IV, V; each 33.3%, 2/6) down to type I, 83.3% (5/6) of who demonstrated the evidence of PD or PD transformed from PR, except for 1 case with PR (case 11). The only cases (case 4) with fluctuations of 4 histologic patterns in our group (from I to V, to

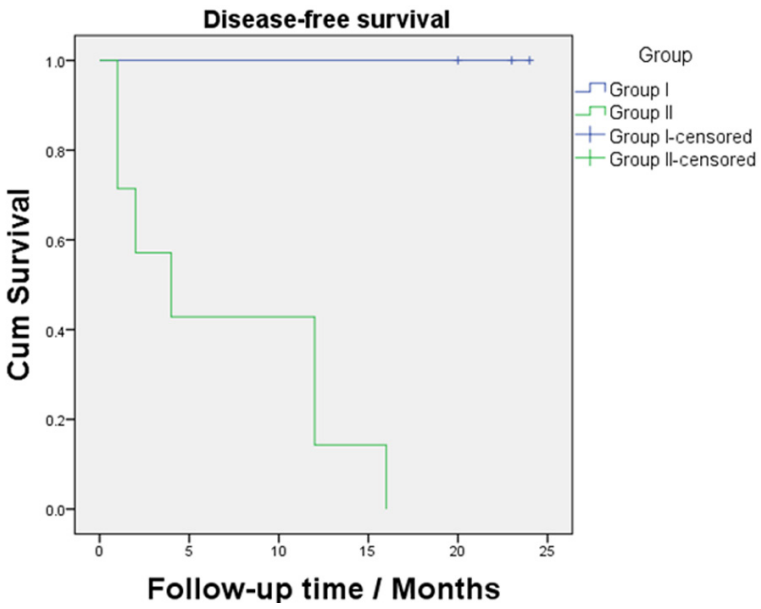

Figure 3. Kaplan-Meier curve showing the DFS of Group I was significantly better than that of Group II (log-rank, *P*=0.009). Group I: patients with any histologic types eventually growing into I or II type until the end of the follow-up; Group II, patients with any histologic types eventually growing into any of the III-V types until the end of the follow-up.

IV, to II) also show a corresponding variation of therapeutic effects from PD to PR.

All follow-up data of the patients after CAR T-cell therapy (range, 1 to 24 months; mean, 10.6 months; median, 10.5 months) were available until this article was written. Five patients (31.3%, 5/16; range, 1 to 6 months; mean, 2.2 months; median, 1 month) were dead, but 3 of them were clinically supposed to succumb to the side effects, such as tumor lysis syndrome (TLS, case 7, 15) or cytokine-release syndrome (CRS, case 18). Four patients experienced a recurrence (25%, 4/16; range, 4 to 16 months; mean, 11 months; median, 12 months), which resulted in clinically multiple pathologic biopsies. The remaining 7 cases (43.8%, 7/16; range, 6 to 22 months; mean, 15.6 months; median, 18 months) were alive with disease and lived through a calm period without any evidence of recurrence or progression. The Chi-square test showed that was not a relationship between each of the histologic types and the status of stable condition or progression to recurrence or death (χ^2=7.267, *P*=0.122), indicating that any single given type cannot predict the prognosis of patients with DLBCL after CAR-T cell therapy. However, the Kaplan-Meier analysis showed that the DFS of Group I was significantly better than that of Group II (log-rank, *P*=0.009; **Figure 3**), indicating that any histologic patterns that grow into any of the III-V types may pursue a better prognosis.

Discussion

The synthetically constructed CAR typically consists of an antigen-recognized extracellular single-chain variable fragment (scFv) that targets a selected antigen (e.g., CD19), a hinge region, and the intracellular domain containing a TCR signaling domain (CD3ζ) [11]. The second intracellular costimulatory-signaling domains are also designed in the second-generation CAR molecules [12]. CAR T-cells can recognize the specific antigen targeted on tumor cells, irrespective of MHC presented by dendritic cells or other antigen-presenting cells [13]. Upon antigen recognition, the downstream activation of CAR-T cells is stimulated followed by specific killing effects [14].

The application of CAR-modified T cells targeting specific tumor cells, as a variety of adoptive cellular immunotherapy, has certainly changed the treatment of B-NHL, especially for aggressive B cell lymphoma [12]. Both single- and multi-center clinical trials with anti-CD19 CAR T-cell therapy have produced high rates of CR in relapsed or refractory (R/R) DLBCL without other available treatment choices [15]. Two commercial CAR T-cell products, that is, axi-cel and tisagenlecleucel, have been approved by the US Food and Drug Administration for R/R DLBCL after 2 or more lines of systemic therapy [12]. Another CAR T-cell product, lisocabtagene maraleuce (liso-cell or JCAR0017), currently under evaluation in clinical trials, is also showing promising results and is the only product that can fix the infused ratio of CD4+ and CD8+ T cells [16].

As a new therapeutic method, CD19-targeted CAR T-cell therapy has been increasingly applied in a few large comprehensive or specialized hospitals. However, more experience in treatment and nursing needs to be accumulat-

ed. It stands to reason that the majority of pathologists are unfamiliar with this terra incognita of morphologic features. Microscopically, the infused T cells are activated and therefore demonstrate somewhat cytologic atypia, such as larger size and irregular nuclei, with usually very high expression of the proliferative index (Ki-67). Furthermore, the proliferated atypical T cells usually give rise to effaced normal nodal structures, angiocentric involvement and lymphoepithelial lesions (LELs). All of these features may easily make the pathologist derive an erroneous diagnosis of T cell lymphomas. In another situation, in the advanced stage of the interaction of CAR T and neoplastic B cells, these significantly reduced components with superimposed proliferated fibroblasts may also lead to an underdiagnosis of a chronic inflammatory process. Furthermore, it becomes difficult when increasing numbers of limited lymphoid tissues are obtained because of the tendency for core-needle biopsies in the clinic. Compared to the specimens after R-CHOP treatment, the diagnosis of DLBCL after CAR T cell therapy seems more challenging, though the former may have a growth pattern similar to type I, and rarely, type IV or V, as well as occasional loss of CD20 expression [17], absence of atypical T cells, and a set number of neoplastic B cells, will not commonly prompt misdiagnosis.

The first summarized 5 histologic features after CD19-targeted CAR T-cell therapy, according to our routine practice, essentially, to some extent, reflected the modalities and phases of the interactions of CAR T cells against B cells. The relatively large quantity of atypical B cells in type I or II often contributes to the diagnosis of DLBCL, with a high diagnostic agreement for most pathologists. However, in the other 3 types, proliferated T cells or fibroblasts may obscure the atypical B cells or even the neoplastic nature, as discussed above. Notably, not only the diagnostic accuracy but also the misdiagnosis agreement were very high in cases of type III, particularly in the case of intestinal lymphomas (case 12). Almost all pathologists rendered a diagnosis for the latter as monomorphic epitheliotropic intestinal T cell lymphoma or intestinal T-cell lymphoma, NOS, due to its transmural infiltration by atypical T cells, prominent enteropathy-like morphologies, focal LELs, and vascular invasion, with very inconspicuous B cell clusters. Essentially, the most practical way to avoid misdiagnosis is an acquaintance of these potential histologic features based on a relevant clinical history of treatment. An active application of genetic detection for BCR and TCR can further confirm or change the preliminary diagnosis because of the very high sensitivity of PCR in hematologic malignancies [18]. In our series, all the specimens demonstrating the presence of rearrangement of BCR but not TCR, irrespective of their histologic types, again indicated the significance of this technique in the differential diagnosis.

The CAR, genetically reprogramed using patients' T cells to specifically target tumor cells, is a major histocompatibility complex (MHC)- and coreceptor (CD4 or CD8)-independent, though the ratios of the latter may correlate with differential expansion, persistence or toxicity [15, 19]. Immunohistochemically, the specimens submitted are supposed to present with varying proportions of CD4+ and CD8+ T cells because the current products we used do not fix the infused ratio of CD4- to CD8-positive T cells, as discussed above [12]. However, all most infiltrated CAR T cells in our series were reactive for CD8 without expression of CD4 or with very scant CD4+ T cells; only 2 cases showed a comparable quantity of CD4+ and CD8+ T cells. These results were similar to the previous study using the same CAR T-cell product (axi-cel) [20]. The cause of this phenomenon is still unknown and warrants further investigations. The majority of T cells expressed TIA-1, but Gran B, seemed rarely positive in our cases. Whether the latter indicates an insignificant effect from the exocytosis pathway of cytologic granules remains unclear, and more studies should be carried out [11].

The pathologic evaluation after CAR T-cell therapy is of importance to provide the pathologic level of evidence, including success or not in CAT T-cell infusion; information in details of the expansion and persistence of T cells; assessment in an individual's therapeutic effectiveness; determination of disease relapse or progression; and monitoring the concrete process of evolution or involvement. In our group, approximately 50% of biopsies were used to assess the treatment or infusion effects, and the remainder were aimed at the determination

of the severity of recurrence. In theory, the pathologic patterns of type III, IV, V seem to be more associated with better prognosis because they represent a dominance of anti-tumor response with fewer neoplastic components. However, just an isolated pathologic result is a narrow view and cannot precisely predict the whole cause of the disease; instead, continuous and regular multiple biopsies could provide more accurate prognostic anticipation. Our study more or less showed that consistent type III, IV, or V may associate with better therapeutic effects and therefore prognosis, but more clinicopathologic studies are needed to confirm this possibility. Moreover, a core needle biopsy for lymph nodes tends to offer limited histologic information; thus, excision, if available, is advocated. The relationship between the given pathologic types demonstrated initially and the long-term prognosis seemed unrelated, but the pathologic transformations from type I or II to type III to V detected by multiple biopsies were likely to be relevant to the remission of disease and a satisfactory prognosis. Therefore, only a combination of clinical and imaging information and serial pathologic features can provide a whole evolution profile and valuable prognostic predictive data.

The mechanism of resistance to CAR-T cell therapy in some patients is complicated; it may be associated with diminished or deficient surface CD19 expression, lack of persistence of CAR-T cells, the tumor burden, the density of the targeted antigens, the status of infused CAR-T cells, the characteristic of the disease per se, as well as the tumor microenvironment [21, 22]. CAR T-cell therapy may bring about severe side effects, including CRS, CAR T cell-related encephalopathy (CRS)/immune effector cell-associated neurotoxicity syndrome (ICANS), TLS, and cytopenia [23, 24]. The relevant management methods for monitoring, grading, or treatment have been documented [23, 25]. The prominent CRS and TLS that occurred in our 3 cases resulted in unsatisfactory treatment effects and unfavorable prognoses. More experience needs to be accumulated for this novel therapy for DLBCL in China.

Conclusions

Collectively, this research first described the clinicopathologic features of diffuse large B cell lymphoma after CD19-targeted CAR T-cell therapy and summarized 5 distinct histologic types. We performed a diagnostic test to further emphasize the potential misdiagnosis pitfalls. To avoid misdiagnosis, familiarity with the features of these 5 patterns and combining the relevant clinical history and genetic tests of BCR and TCR rearrangement are warranted. A single pathologic type seems to not precisely predict the long-term treatment effects and prognosis, but a combination of these types from multiple biopsies may indicate the changes of disease, that is, consistent type III to V may suggest a favorable process, contrary to types I and II, but we still need more cases and upgraded studies to reveal their concrete relationships.

Acknowledgements

This work is supported by the Shanghai Science and Technology commission (17ZR1417500); the National Key Research and Development Program of China (YFC201701101001); and Shanghai Science and Technology Development fund (19MC1911000).

Disclosure of conflict of interest

None.

Address correspondence to: Drs. Chaofu Wang and Jun Zhou, Department of Pathology, Ruijin Hospital, Shanghai Jiaotong University School of Medicine, No. 197, 2nd Ruijin Road, Huangpu District, Shanghai, China. E-mail: wangchaofu@126.com (CFW); zhoujun2006305@126.com (JZ)

References

[1] Li S, Young KH and Medeiros LJ. Diffuse large B-cell lymphoma. Pathology 2018; 50: 74-87.

[2] Swerdlow SH, Campo E, Harris NL, Jaffe ES, Pileri SA, Stein H and Thiele J. WHO classification of tumours of haematopoietic and lymphoid tissues. Lyon: IARC; 2017.

[3] Coiffier B, Thieblemont C, Van Den Neste E, Lepeu G, Plantier I, Castaigne S, Lefort S, Marit G, Macro M, Sebban C, Belhadj K, Bordessoule D, Ferme C and Tilly H. Long-term outcome of patients in the LNH-98.5 trial, the first randomized study comparing rituximab-CHOP to standard CHOP chemotherapy in DLBCL patients: a study by the Groupe d'Etudes des Lymphomes de l'Adulte. Blood 2010; 116: 2040-2045.

[4] Mondello P and Mian M. Frontline treatment of diffuse large B-cell lymphoma: beyond R-CHOP. Hematol Oncol 2019; 37: 333-344.

[5] Nowakowski GS, Blum KA, Kahl BS, Friedberg JW, Baizer L, Little RF, Maloney DG, Sehn LH, Williams ME, Wilson WH, Leonard JP and Smith SM. Beyond RCHOP: a blueprint for diffuse large B Cell Lymphoma Research. J Natl Cancer Inst 2016; 108: djw257.

[6] Skrabek P, Assouline S, Christofides A, MacDonald D, Prica A, Sangha R, Matthews BA and Sehn LH. Emerging therapies for the treatment of relapsed or refractory diffuse large B cell lymphoma. Curr Oncol 2019; 26: 253-265.

[7] Maus MV and Levine BL. Chimeric antigen receptor T-cell therapy for the community oncologist. Oncologist 2016; 21: 608-617.

[8] Makita S, Yoshimura K and Tobinai K. Clinical development of anti-CD19 chimeric antigen receptor T-cell therapy for B-cell non-Hodgkin lymphoma. Cancer Sci 2017; 108: 1109-1118.

[9] Fleiss JL. Measuring nominal scale agreement among many raters. Psychological Bulletin 1971; 76: 378-382.

[10] Hans CP, Weisenburger DD, Greiner TC, Gascoyne RD, Delabie J, Ott G, Muller-Hermelink HK, Campo E, Braziel RM, Jaffe ES, Pan Z, Farinha P, Smith LM, Falini B, Banham AH, Rosenwald A, Staudt LM, Connors JM, Armitage JO and Chan WC. Confirmation of the molecular classification of diffuse large B-cell lymphoma by immunohistochemistry using a tissue microarray. Blood 2004; 103: 275-282.

[11] Benmebarek MR, Karches CH, Cadilha BL, Lesch S, Endres S and Kobold S. Killing mechanisms of chimeric antigen receptor (CAR) T cells. Int J Mol Sci 2019; 20: 1283.

[12] Chavez JC, Bachmeier C and Kharfan-Dabaja MA. CAR T-cell therapy for B-cell lymphomas: clinical trial results of available products. Ther Adv Hematol 2019; 10: 2040620719841581.

[13] Dai H, Wang Y, Lu X and Han W. Chimeric antigen receptors modified T-cells for cancer therapy. J Natl Cancer Inst 2016; 108: djv439.

[14] Zhao L and Cao YJ. Engineered T cell therapy for cancer in the clinic. Front Immunol 2019; 10: 2250.

[15] Turtle CJ, Hanafi LA, Berger C, Gooley TA, Cherian S, Hudecek M, Sommermeyer D, Melville K, Pender B, Budiarto TM, Robinson E, Steevens NN, Chaney C, Soma L, Chen X, Yeung C, Wood B, Li D, Cao J, Heimfeld S, Jensen MC, Riddell SR and Maloney DG. CD19 CAR-T cells of defined CD4+:CD8+ composition in adult B cell ALL patients. J Clin Invest 2016; 126: 2123-2138.

[16] Qin JS, Johnstone TG, Baturevych A, Hause RJ, Ragan SP, Clouser CR, Jones JC, Ponce R, Krejsa CM, Salmon RA and Ports MO. Antitumor potency of an Anti-CD19 chimeric antigen receptor T-cell therapy, lisocabtagene maraleucel in combination with ibrutinib or acalabrutinib. J Immunother 2020; 43: 107-120.

[17] Maeshima AM, Taniguchi H, Nomoto J, Maruyama D, Kim SW, Watanabe T, Kobayashi Y, Tobinai K and Matsuno Y. Histological and immunophenotypic changes in 59 cases of B-cell non-Hodgkin's lymphoma after rituximab therapy. Cancer Sci 2009; 100: 54-61.

[18] Gazzola A, Mannu C, Rossi M, Laginestra MA, Sapienza MR, Fuligni F, Etebari M, Melle F, Sabattini E, Agostinelli C, Bacci F, Sagramoso Sacchetti CA, Pileri SA and Piccaluga PP. The evolution of clonality testing in the diagnosis and monitoring of hematological malignancies. Ther Adv Hematol 2014; 5: 35-47.

[19] Wang Y, Luo F, Yang J, Zhao C and Chu Y. New chimeric antigen receptor design for solid tumors. Front Immunol 2017; 8: 1934.

[20] Spiegel JY, Sahaf B, Hossain N, Frank MJ, Claire G, Abramian M, Latchford T, Villa B, Cancilla J, Oak J, Natkunam Y, Long SR, Arai S, Johnston LJ, Lowsky R, Meyer EH, Muffly LS, Negrin RS, Rezvani AR, Shizuru JA, Weng WK, Kong KA, Mackall CL and Miklos DB. Elevated axicabtagene ciloleucel (CAR-19) expansion by immunophenotyping is associated with toxicity in diffuse large B-cell lymphoma. Blood 2018; 132: 576-576.

[21] Cheng J, Zhao L, Zhang Y, Qin Y, Guan Y, Zhang T, Liu C and Zhou J. Understanding the mechanisms of resistance to CAR T-cell therapy in malignancies. Front Oncol 2019; 9: 1237.

[22] Singh N, Orlando E, Xu J, Xu J, Binder Z, Collins MA, O'Rourke DM and Melenhorst JJ. Mechanisms of resistance to CAR T cell therapies. Semin Cancer Biol 2020; 65: 91-98.

[23] Neelapu SS. Managing the toxicities of CAR T-cell therapy. Hematol Oncol 2019; 37 Suppl 1: 48-52.

[24] Brudno JN and Kochenderfer JN. Toxicities of chimeric antigen receptor T cells: recognition and management. Blood 2016; 127: 3321-3330.

[25] Yanez L, Sanchez-Escamilla M and Perales MA. CAR T cell toxicity: current management and future directions. Hemasphere 2019; 3: e186.